Science of the Total Environment xxx (xxxx) xxx

Contents lists available at ScienceDirect

Science of the Total Environment

journal homepage: www.elsevier.com/locate/scitotenv

Seasonal variations in water uptake and transpiration for plants in a karst critical zone in China

Hamid M. Behzad [a], Muhammad Arif [b,c], Shihui Duan [a], Alireza Kavousi [d], Min Cao [a,e], Jiuchan Liu [a], Yongjun Jiang [a,*]

[a] Chongqing Key Laboratory of Karst Environment & School of Geographical Sciences, Southwest University, Chongqing 400715, China
[b] Key Laboratory of Eco-Environments in the Three Gorges Reservoir Region (Ministry of Education), Chongqing Key Laboratory of Plant Resource Conservation and Germplasm Innovation, School of Life Sciences, Southwest University, Chongqing 400715, China
[c] Biological Science Research Center, Academy for Advanced Interdisciplinary Studies, Southwest University, Chongqing 400715, China
[d] Institute of Groundwater Management, Technische Universität Dresden, 01069 Dresden, Germany
[e] School of Earth Sciences, Yunnan University, 650500, China

HIGHLIGHTS

- This study was conducted using $\delta^{18}O$, $\delta^{2}H$, $\delta^{13}C$, WUE_i, transpiration (E_t), and rooting depth.
- Water uptake in habitats shifts seasonally due to limited water supply in surface pools.
- E_t and WUE_i variations in habitats are influenced by seasonal shifts in water uptake.
- Regulation of E_t and WUE_i is stricter in RDH than in SDH due to lower soil water supply.
- E_t, WUE_i, and water-uptake vary seasonally among species with different rooting depths.

GRAPHICAL ABSTRACT

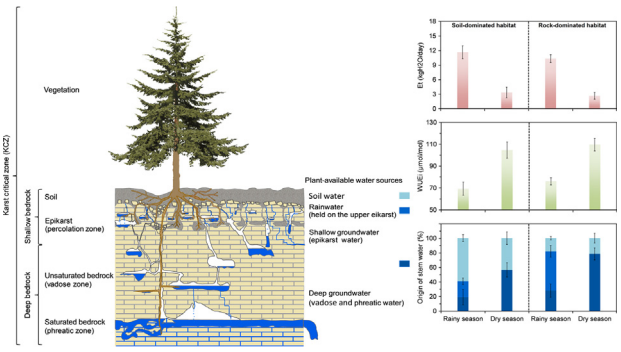

ARTICLE INFO

Editor: Fernando A.L. Pacheco

Keywords:
Plant-available water source
Transpiration dynamic
Ecohydrological niche
Forest woody plant
Karst critical zone

ABSTRACT

Despite substantial drought conditions in the karst critical zone (KCZ), the KCZ landscapes are often covered with forest woody plants. However, it is not well understood how these plants balance water supply and demand to survive in such a water-limited environment. This study investigated the water uptake and transpiration relationships of four coexisting woody species in a subtropical karst forest ecosystem using measurements of microclimate, soil moisture, stable isotopes ($\delta^{18}O$, $\delta^{2}H$, and $\delta^{13}C$), intrinsic water-use efficiency (WUE_i), sap flow, and rooting depth. The focus was on identifying differences within- and between-species across soil- and rock-dominated habitats (SDH and RDH) during the rainy growing season (September 2017) and dry season (February 2018). Species across both habitats tended to have higher transpiration with lower WUE_i during the rainy season and lower transpiration with higher WUE_i during the dry season. Compared to those in the SDH, species in the RDH showed lower transpiration with higher WUE_i in both seasons. The dominant water sources were soil water and rainwater for supporting rainy-season transpiration in the SDH and RDH, respectively, and groundwater was the main water source for supporting dry-season transpiration in both habitats. A clear ecohydrological niche differentiation was also revealed among species. Across both habitats, shallower-rooted species with higher soil-water uptake, compared to deeper-rooted species

* Corresponding author.
E-mail address: jiangjyj@swu.edu.cn (Y. Jiang).

http://dx.doi.org/10.1016/j.scitotenv.2022.160424
Received 29 September 2022; Received in revised form 13 November 2022; Accepted 19 November 2022
Available online xxxx

with higher groundwater uptake, showed higher transpiration and lower WUE_i during the rainy season and vice versa during the dry season. This study provides integrated insights into how forest woody plants in the KCZ regulate transpiration and WUE_i in response to drought stress through interactions with seasonal water sources in the environment.

1. Introduction

In many forest ecosystems, plant water availability is affected by seasonal variations in rainfall (McCole and Stern, 2007; Wang et al., 2017; Ding et al., 2021; Behzad et al., 2022). This, in turn, shapes the water uptake and transpiration strategies that plants can adopt to cope with drought (water) stress (Leo et al., 2014; Obojes et al., 2018; Wu et al., 2021). A better knowledge of the diversity of ecophysiological responses to drought stress is essential for forest development and sustainability (McDowell et al., 2011; Anderegg et al., 2019; Brum et al., 2019; Wang et al., 2021).

A critical zone (CZ), including the karst critical zone (KCZ), comprises a set of biophysical layers that extend from the top of the forest canopy downward through the soil and into the surface and subsurface water-bearing bedrock (Dawson et al., 2020; Fig. 1). Throughout the context of the KCZ, which is inherently sensitive to seasonal variations in water supply associated with changing rain inputs, drought stress does not occur uniformly, primarily because of the extremely high contextual heterogeneity (Nardini et al., 2020; Deng et al., 2021; Behzad et al., 2022). For example, in rock-dominated karst habitats, compared to soil-dominated karst habitats, the soil is poorly developed and rocky, which considerably limits water storage capacity in the near-surface for plant uptake (Chen et al., 2011; Nie et al., 2019; Carrière et al., 2019). Another important driver of drought stress in the KCZ is the large water infiltration capacity of the surface fractured bedrock (Estrada-Medina et al., 2013; Liu and She, 2020), which can explain the rarely observed surface runoff and streams in the KCZs (Gregory et al., 2009; Yang et al., 2016). For these reasons, KCZ landscapes are ostensibly not well-suited for vegetation development. However, they are often covered with forests (Zhao and Wang, 2018; Carrière et al., 2020; Liu et al., 2021a).

The availability of groundwater and deep rooting are two determining factors for maintaining the growth and survival of plants in the KCZs (Fan, 2015; Richter and Billings, 2015; Schwinning, 2020; Liu et al., 2021b). As field-based studies have demonstrated, water supply in groundwater pools (either epikarst or phreatic) is less affected by the seasonal or short-term variations of rain inputs (Rose et al., 2003; Huang et al., 2011; Hahm et al., 2019, 2022). Therefore, these water pools can serve as stable hydrologic refugia for plants, especially during rainless conditions when the soil becomes increasingly dry (McLaughlin et al., 2017; Ackerly et al., 2020). However, access to groundwater supply is impossible for all plants, including shallow-rooted plants (Dawson and Pate, 1996; Teodoro et al., 2019). Plant access may also prove difficult due to the limited development of bedrock fractures that exclude deep rooting (Estrada-Medina et al., 2013;

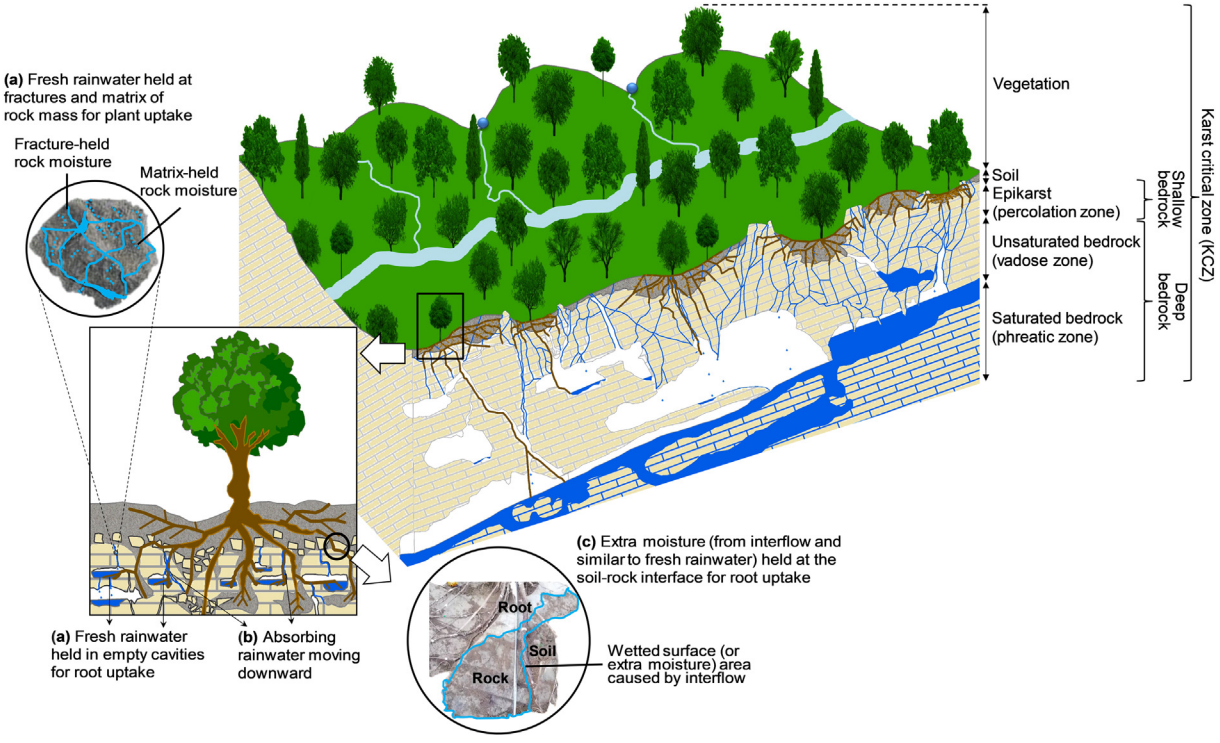

Fig. 1. A conceptual sketch of water sources potentially available to forest trees in a karst critical zone (KCZ). The KCZ includes a set of biophysical layers (defined along the right-hand margin) that extend from the top of the forest canopy to where groundwater is actively circulating in the saturated bedrock (the upper phreatic zone) (Dawson et al., 2020). While the KCZ structurally varies from region to region depending on the geological structure and lithology, climate, and vegetation type, it generally supplies three potential water sources within a complex and heterogeneous context for plant uptake: (1) soil water that is supplied at the different depths of the soil zone; (2) groundwater that is supplied in two zones of the shallow bedrock (epikarst zone) and deep bedrock (vadose and phreatic zones); and (3) rainwater that is supplied as a seasonal reserve in the uppermost layer of the shallow bedrock (the upper epikarst). As illustrated by three schemas, plants may take up the rainwater that retains its initial (isotope) composition from (a) a temporary pool (i.e., from recent rainwater temporarily held in the fractures and cavities with relatively narrow bottoms), (b) a mobile pool (i.e., from rainwater moving downward) on the upper epikarst, and from (c) a substrate (i.e., through water or residual moisture related to the generation of interflow) at the soil–bedrock interface.

Nardini et al., 2020). Furthermore, some studies have indicated that facilitating water uptake from depth is impossible without consuming metabolic energy (Jiang et al., 2020; Wu et al., 2021). Besides, plants may have to resort to alternative mechanisms to survive drought. Accordingly, plants might decrease their transpiration and increase their water-use efficiency (WUE_i) as drought stress intensifies (Craven et al., 2013; Wang et al., 2021). Other drought survival mechanisms include decreasing stomatal conductance and photosynthetic rates (Klein et al., 2011; Maxwell et al., 2018) and the formation of leaves with well-developed epidermal hairs and thicker cuticles or waxy layers (Barbeta and Peñuelas, 2016). However, despite recent advances, climate-mediated, ecophysiological interactions have received less attention from the KCZ perspective, especially in well-karstified environments.

By taking advantage of the heterogeneous nature of soil- and rock-dominated habitats (SDH and RDH) across a typical KCZ forest ecosystem located in southwest China, this study investigates: (1) how forest woody species across both habitat types regulate transpiration and water loss according to drought-induced seasonal shifts in water supply from different available source pools, including rainwater, soil water, and groundwater; (2) whether greater use of groundwater contributes to increased transpiration rate and reduced drought stress level in species; and (3) the mechanisms behind seasonal water uptake strategies for the regulation of transpiration and whether they vary between and within species. Water shares from different water sources supplied to the environment were quantified, and WUE_i values and transpiration rates for four coexisting woody species across habitats between seasons were determined. The relationships between groundwater use, WUE_i, and transpiration were also examined to ascertain each species' seasonal physiological response in both habitat types. It was hypothesized that: (1) transpiration is limited in the dry season compared to that in the rainy season due to decreases in the near-surface water supply; (2) transpiration for species in the RDH is reduced compared to those in the SDH due to lower availability of soil water; (3) use of groundwater during the dry season helps to reduce drought stress in species of both habitat-types; and (4) the pattern of water uptake and transpiration is different among species due to differences in maximum rooting depth. Accordingly, water uptake and transpiration rates are higher in species with deeper roots.

2. Materials and methods

2.1. Study area

The study area consists of a typical karst depression surrounded by mountains with an area of 39 km^2 that is situated in northwest Chongqing, southwest China (29°40′30″–29°48′10″N, 106°23′15″–106°28′05″E; Fig. 2). This region has a subtropical, humid, monsoon climate with an annual mean temperature and precipitation of 18 °C and 1200 mm, respectively. The rainy season occurs between April and October, receiving 75–85 % of the total rainfall. The dry season occurs between November and March, receiving 15–25 % of the total rainfall, and is characterized by a 4–5-month seasonal drought.

Lithologically, the karst depression is composed almost entirely of limestone ($CaCO_3$) with minor impurities, such as dolomite ($CaMg(CO_3)_2$). Geologically, a dense network of vertical open fractures has developed in the limestone bedrock of the karst depression. The thickness of the limestone bedrock ranges from 500 to 700 m (Liu et al., 2019). In the bedrock structure, two distinct hydrological subzones are present: an epikarst zone, or the near-surface fractured zone, characterized by a dominant diffuse flow system, and a phreatic or saturated zone characterized by a dominant conduit flow system (Lv et al., 2022). The layer thickness of the epikarst zone in the region ranges from approximately 5 m on hillslopes to approximately 8 m in flatter areas. The matrix porosity of the epikarst zone varies between 8 and 45 %, which is lower than that of the shallow soil layer (46–53 %). The potential available water storage (PAWS) of the epikarst zone is 333–1690 m^3/ha and much higher than that of the shallow soil layer, which measures 0–143 m^3/ha (see Tables S1 and S2 for additional details regarding other physical characteristics of the region's epikarst and soil, respectively, reported by Chongqing Nanjiang Geological Engineering Survey and Design Institute (CNGESDI), 2015; Lv et al., 2022). This water reserve of epikarst can remain available to the plants longer than the soil water reserve, especially during long-lasting periods of water stress (Estrada-Medina et al., 2013). According to field measurements collected during the last 5 years (2017–2022), the region's epikarst water storage is drained by three permanent springs with an average annual flow of nearly 10 L/s. In contrast, the water storage of the phreatic

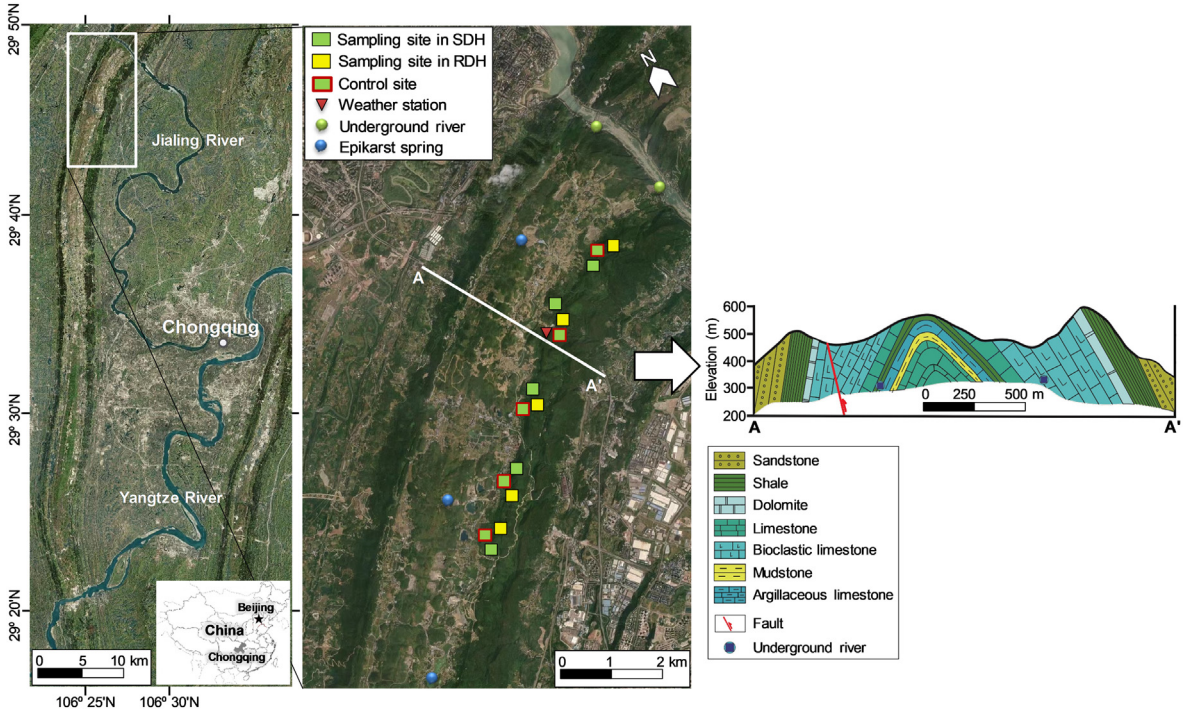

Fig. 2. The location, sampling sites, hydrologic observation points, and geological cross-section of the study area.

zone is mainly drained by three outlets of two underground rivers with an annual average flow of nearly 40 L/s (Li et al., 2021). The continuous high-resolution monitoring of discharges from underground rivers as well as the rainfall during the last 5 years (2017–2022) shows that peak flow rates at the underground river outlets often occur between one and 11 h after the biggest volume of rainfall (see Table S3 for details). This indicates that the timing, distribution, and volume of water flow in the phreatic zone are highly irregular, primarily because of the high karstification (Lv et al., 2022). Furthermore, this could explain for the scarcity of surface runoff generated in the region (Li et al., 2021).

2.2. Characteristics of the habitats

Two habitat types with different soil characteristics were identified in the study area: soil-dominated habitat (SDH) and rock-dominated habitat (RDH), which account for >70 % and <30 % of the surface area, respectively. Across the SDH, the soil has a continuous, thin layer (40–50 cm) that covers most of the underlying fractured bedrock outcrops and consists of 41 to 54 % coarse particles (loam and sandy clay loam, according to U. S. Department of Agriculture (USDA) and Natural Resources Conservation Service (NRCS), 2012). According to Estrada-Medina et al. (2013), the PAWS of SDH soil ranges between 118 and 143 m^3/ha (Table S2). Across the RDH, the soil has a discontinuous cover with a variable thickness (0–65 cm) that is interrupted by numerous rocky outcrops. It is found around the base of individual trees and forest stands or in some flat patches. RDH soil contains 57 to 66 % coarse particles (sandy loam, according to U. S. Department of Agriculture (USDA) and Natural Resources Conservation Service (NRCS), 2012); the PAWS of RDH soil ranges between 0 and 34 m^3/ha (Table S2). In terms of vegetation, both habitat types are covered by native woody species, dominated by shrub species of *Berchemia polyphylla* (BP) and *Viburnum chinshanense* (VC), and tree species of *Citrus reticulate* (CR) and *Fraxinus chinensis* (FC). These species were found to coexist with contrasting life forms, leaf habits, and rooting depths (see details in Table 1) and, thus, were targeted for this study.

2.3. Potential water sources supplied for the plants in the environment

Based on ecohydrological evidences from recent studies (Liu et al., 2019; Cao et al., 2020; Wu et al., 2021) and on direct measurements of rooting depth from a previous study conducted in the same region (Liu, 2018; see details in Table 1 and Section 4.2), three potential, plant-available water sources were identified: (1) soil water supplied at two depths of 0–20 cm (upper soil layer) and 20–40 cm (lower soil layer), which are separated hydrologically (water content) and isotopically ($\delta^{18}O$ and $\delta^{2}H$) into two distinct source pools (see additional details in Sections 3.1 and 3.2); (2) groundwater supplied in two zones of the shallow bedrock, or epikarst, and deep bedrock, both vadose and phreatic, which differ hydrologically (in terms of distribution and volume of water) but pool, isotopically, into a common water source for plant use and are hereinafter referred to collectively as groundwater; and (3) rainwater supplied in the uppermost layer of the shallow bedrock, or the upper epikarst, which is often available as a temporary reserve during the rainy season (see details in Supplementary material Fig. S3 and Notes S1 and S2). Through comparing the isotopic signals of stem and source waters (Figs. 4, 5, S1, and S2, described in Sections 3.2 and 3.3), which was also validated by the IsotopeR results (Fig. 6, described in Section 3.4), it was found that the rainwater, responsible for supporting growing-season transpiration, most likely came from rainfall and interflow that occurred in September 2017 rather than from rainfall and interflow that occurred before. Since the rainfall and interflow events that occurred in September had small isotopic variations and the values were similar to each other, the merged arithmetic mean was used to represent the "rainwater" signal during the rainy season (Figs. 4, 5, S1a, and S2a). During the dry season (February 2018), no rainfall or interflow occurred above the threshold for plant uptake with all major rainfall events measuring <5 mm (Fig. 3a), which did not result in the generation of interflow as well.

2.4. Sampling

Plant and soil sampling was conducted across 15 approximately 70 × 70 m sites with similar altitudes around 430–500 m above sea level (asl) and slopes between 10 and 30 %. Ten sites were established within the SDH, and the other five were established within the RDH. Most of the sites were dominated by two native woody shrub species (BP and VC) and two native tree species (CR and FC). The stand structures of each site, including leaf habit, diameter at breast height, and plant size were investigated in June and July 2017 (Table 1). Moreover, the maximum rooting depth was obtained from previous observations made in 46 pits excavated in the study area (Liu, 2018), current observations made in roadcuts, and also inquiries from 13 local professional experienced drillers. More information on the maximum rooting depth of each woody species and also on the number of pits excavated per species per individual is presented in Table 1.

Three to four individuals, including a minimum of two replicates of each species, were selected if the target species was present at the sampling site for stem water and leaf isotopic measurements. All individuals across the sites were marked for ecophysiological measurements during September 2017 and February 2018 (late rainy and dry seasons, respectively). A total of 206 individuals (136 from the SDH sites and 70 from the RDH sites) were sampled during each season (Table 1). The selected individuals in each study site covered almost the entire surface area of that site. For the measurements of stem water isotopic signatures, comprising $\delta^{18}O$ and $\delta^{2}H$ measurements, three to five sun-exposed suberized twigs were collected from the canopy of individuals of each target species across the sites during both seasons. All leaves and bark-like tissues were carefully removed from the twigs with sterilized razor blades to minimize the risk of back-diffusion of isotopically enriched water (Ehleringer and Dawson, 1992). Chipped stems were immediately placed in glass-capped vials, wrapped in parafilm, and kept frozen to prevent evaporation before isotope analysis could be conducted. For the measurements of leaf isotopic signatures, comprising $\delta^{13}C$ measurements, at least 10 mature, intact, sunlit, upper canopy leaves were collected from all the marked individuals of each target species across the sites during both seasons. All leaves sampled were subsequently dried in an oven at 70 °C to a constant weight and then were ground to a fine

Table 1
Main characteristics of the four woody plant species targeted in the study.

Species	Abbreviation	Family	Leaf phenology	$N_{Stem\ water\ \&\ leaf\ measurements}$		$N_{Sap\ flow\ measurements}$		Averageheight (m)	Average DBH (cm)	Rooting depth (m)[a]	
				SDH	RDH	SDH	RDH			SDH	RDH
Berchemia polyphylla	BP	Rhamnaceae	Deciduous Shrub	32	13	10	6	4.43 ± 1.15	12.26 ± 2.03	3–4	2–6
Viburnum chinshanense	VC	Adoxaceae	Evergreen shrub	40	22	17	10	5.30 ± 1.03	21.49 ± 1.64	9–19	13–25
Citrus reticulate	CR	Rutaceae	Evergreen tree	21	12	11	7	4.87 ± 1.51	15.12 ± 1.25	3–7	5–8
Fraxinus chinensis	FC	Oleaceae	Deciduous tree	43	23	14	12	6.64 ± 0.78	27.57 ± 1.92	11–28	17–36

$N_{Stem\ water\ \&\ leaf\ measurements}$, $N_{Sap\ flow\ measurements}$, sampling number for the stem water and leaf, and sap flow measurements, respectively. DBH, diameter at breast height. SDH, RDH, soil- and rock-dominated habitats, respectively. Species average values ± SE are shown.

[a] The maximum rooting depth was obtained from previous observations made in 46 pits excavated in the study area (Liu, 2018), current observations made in roadcuts, and also inquiries from 13 local professional experienced drillers.

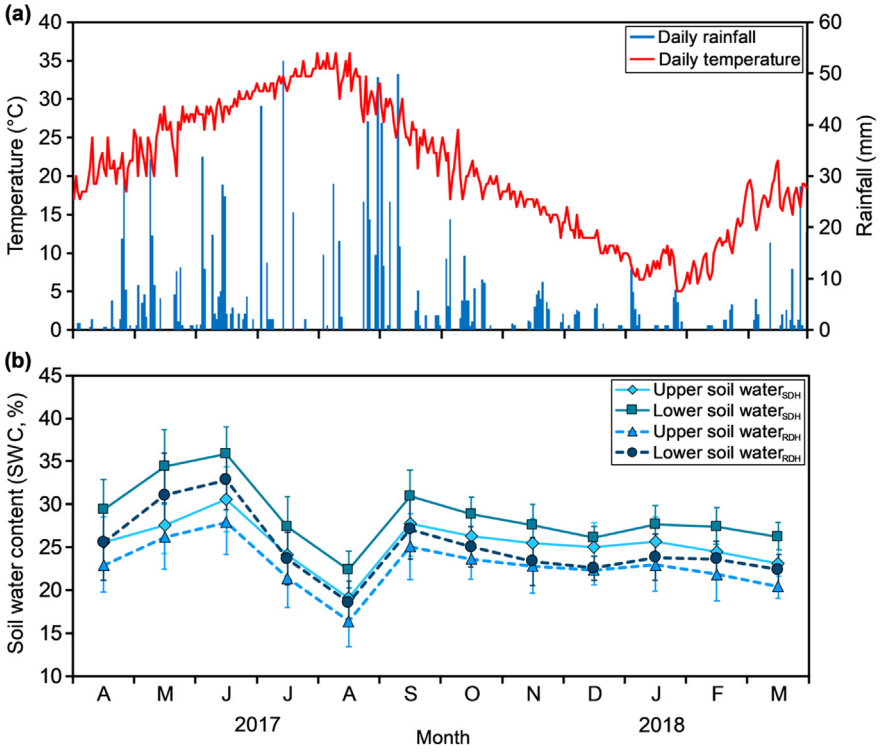

Fig. 3. Variations in (a) daily temperature (°C) and daily rainfall (mm) and (b) monthly soil water content (SWC, %) of various soil layers across the soil- and rock-dominated habitats (SDH and RDH) over a hydrological year (April 2017–March 2018).

powder for isotope analysis. During each season, two replicated 100-cm gas samples were collected using 300-mL air bags installed in each of the five control sites in the study area to measure air CO_2 concentration for $\delta^{13}C_a$ determination (see Eqs. (5) and (6)). To accurately represent the air of the upper canopy, air bags were installed at an altitude of approximately 20–35 m higher than the canopy of the control sites.

To measure sap flow for transpiration estimation, 87 out of the 206 previously marked individuals across the pre-selected sites per habitat (52 and 35 replicated individuals across the SDH and RDH sites, respectively) were instrumented with thermal dissipation probes, as described by Granier (1987). The selected individuals covered almost the entire surface area of the study sites. To avoid direct sunlight, the probes were installed on the north side of the trunks of each individual at breast height (1.3 m). All measurements were logged at 15 min intervals throughout the day and night from April 19 to October 24, 2017, during the rainy growing season, and from October 25, 2017, to March 27, 2018, during the dry season. To estimate stand-level transpiration, the obtained sap flow rates were normalized to minimize differences among individuals of each species, as described by Du et al. (2011). They then were scaled to the species level based on sapwood basal area for individuals of the same species (see Eqs. (7) and (8)).

For soil sampling, four soil samples were collected using a 5-cm-diameter hand probe from each site across depths of 0–20 and 20–40 cm, with $n = 2$ per depth. The samples were subsequently prepared for soil water content analysis monthly (April 2017–March 2018) and soil water isotopic analysis ($\delta^{18}O$ and $\delta^{2}H$) seasonally (September 2017 and February 2018). A total of 1080 soil samples ($n = 30$ and 15 per depth per month across the sites established in the SDH and RDH, respectively) were gathered to measure the gravimetric soil water content (SWC, %), and 180 soil samples (n = 30 and 15 per depth per season across the sites established in the SDH and RDH, respectively) were gathered to measure soil water isotopic signatures. All collected samples were immediately placed in glass-capped vials and preserved the same way as the plant samples. Five control sites established across the SDH were considered (Fig. 2) for continuous monitoring of soil water content in the two mentioned depth ranges every 15 min during a hydrological year (April 2017–March 2018) (Fig. 3b).

The groundwater isotopic signatures ($\delta^{18}O$ and $\delta^{2}H$) were collected seasonally from the outlets ($n = 2$ per outlet per season) of three underground rivers as well as three epikarst springs in the study area (Fig. 2). All samples collected ($n = 24$) were sealed and stored for the isotope analysis in the same manner as the plant and soil samples.

The rainwater isotopic signatures ($\delta^{18}O$ and $\delta^{2}H$) during the rainy season were obtained from rainfall and interflow that occurred in September 2017. As previously mentioned in Section 2.3, during the dry season (February 2018), no significant rainfall or interflow occurred that could be collected and subsequently measured. September rainwater samples were collected from eight major daily rainfall events using a rain gauge directed to a barrel placed in the five control sites. Following standard protocols (IAEA, 2014), each rainwater collecting barrel was installed in a pit sheltered from light and equipped with an atmospheric pressure capillary to minimize the isotopic enrichment effect of evaporation (see Fig. S4). Simultaneously, interflow water samples were collected 40 cm below the surface using a small lysimeter directed to a barrel placed in each control site similar to that used in the rainwater collection system (Fig. S4). Only five out of the eight major rainfall events during September resulted in interflow generation. All samples of rainwater ($n = 80$, including two replicates per control site) and interflow water ($n = 75$, including three replicates per control site) were preserved in the same way as the plant and soil samples.

The meteorological data, including rainfall and air temperature, was measured once every 15 min during the hydrological year using a portable weather station installed in an open place with an altitude of approximately 20–35 m higher than the canopy in the sampling sites (Fig. 2).

2.5. Isotopic analyses

Water was extracted from the soil and plant stem samples through cryogenic vacuum distillation (West et al., 2006; Orlowski et al., 2013). Only samples with a water recovery rate of over 99 % were utilized for isotope

analysis. Unfractionated water samples were transferred into 2-mL sealed brown bottles and stored at 4 °C until use. The $\delta^{18}O$ and $\delta^{2}H$ values of all stem and source water samples were determined utilizing a liquid water isotope analyzer (LWIA; DLT-100, LGR Inc.; Wassenaar et al., 2014). Organic compounds, such as methanol and ethanol, could easily contaminate the extracted stem water samples, leading to errors in the measured $\delta^{18}O$ and $\delta^{2}H$ values (West et al., 2010; Millar et al., 2018). To account for this, the $\delta^{18}O$ and $\delta^{2}H$ values from these samples were first examined for possible spectral interferences utilizing the spectral contamination processing software (LGR, Inc.; Wu et al., 2016). The isotope data from all stem water samples were modified using a specific standard curve provided by Los Gato's engineers (Schultz et al., 2011). All values of $\delta^{18}O$ and $\delta^{2}H$ can be expressed in delta notation (δ) with the unit of permil (‰) as follows:

$$\delta\ (‰) = \left(R_{sample}/R_{standard} - 1\right) \times 1000 \quad (1)$$

where $R_{standard}$ and R_{sample} are the absolute isotope ratios ($^{18}O/^{16}O$ and $^{2}H/^{1}H$) of the standard reference material (Standard Mean Ocean Water, SMOW) and the sample, respectively (Gonfiantini, 1978; Ehleringer et al., 2000). The standard deviation for replicate measurements was reported to be less than ±0.1 ‰ for $\delta^{18}O$ and ± 0.3 ‰ for $\delta^{2}H$.

An elemental analyzer coupled with an isotope-ratio mass spectrometer (EA-IRMS, USA) was used to measure the leaf $\delta^{13}C$ value. The standard deviation for replicate measurements was reported to be less than ±0.1 ‰ Vienna Pee Dee Belemnite (VPDB) standard.

2.6. Data analysis

A comprehensive Bayesian mixing model (IsotopeR; Hopkins and Ferguson, 2012) was employed to estimate the relative share of potential water sources to the total plant water uptake. In this model, like other mixing models, isotope signatures of $\delta^{18}O$ and $\delta^{2}H$ are used to determine the relative share (*f*) of multiple water sources (1, 2, 3…n) to a mixture of stem water (*m*) according to the following mass balance equations (Schwarcz, 1991):

$$\delta^{18}_{m}O = f_1\,\delta^{18}_{1}O + f_2\,\delta^{18}_{2}O + f_3\,\delta^{18}_{3}O + \ldots + f_n\,\delta^{18}_{n}O \quad (2)$$

$$\delta^{2}_{m}H = f_1\,\delta^{2}_{1}H + f_2\,\delta^{2}_{2}H + f_3\,\delta^{2}_{3}H + \ldots + f_n\,\delta^{2}_{n}H \quad (3)$$

$$f_1 + f_2 + f_3 + \ldots + f_n = 1 \quad (4)$$

where f_i defines the relative share, and $\delta^{18}_{i}O$ and $\delta^{2}_{i}H$ represent the isotope signatures for each water source. To minimize the uncertainty of the estimates of each source's shares, several sensitivity analyses were conducted to test the relative effects of (1) sample sizes, (2) the value of inferences for different sources, (3) the isotopic signature difference among the sources, (4) isotopic signature standard deviations (SD) in the mixture and source populations, and (5) analytical SD (SD among replicated samples). Furthermore, in this model, corrections associated with the isotopic correlation coefficients for the mixtures and sources were included as well as the errors associated with measurement for each observation. All estimates were reported as an average ± 1SD for the individual sources at the population level. More details about the sensitivity analyses and the uncertainties associated with the model input data have been fully addressed in previous work (Wu et al., 2021).

Intrinsic water-use efficiency (WUE_i) was calculated using species mean $\Delta^{13}C$ (photosynthetic ^{13}C discrimination) according to a leaf-scale model of C_3 photosynthetic isotope discrimination (Farquhar et al., 1989):

$$WUE_i = \frac{C_a\left(b - \Delta^{13}C\right)}{1.6(b - a)} \quad (5)$$

where C_a (ppm) is the CO_2 concentration in the ambient air, *a* is the $^{13}CO_2$ fractionation due to diffusion through stomata pores (4.4 ‰; O'Leary, 1981), and *b* is the fractionation during carboxylation by the CO_2-fixing enzyme Rubisco (27 ‰; Farquhar and Richards, 1984). C_a measured during September 2017 and February 2018 were 384 and 460 ppm, respectively. $\Delta^{13}C$ was estimated from the $^{13}C/^{12}C$ ratio in leaves according to Farquhar and Richards (1984):

$$\Delta^{13}C = \frac{\delta^{13}C_a - \delta^{13}C_p}{1 + {}^{\delta^{13}C_p}/_{1000}} \quad (6)$$

where $\delta^{13}C_a$ is the $\delta^{13}C$ value of CO_2 in ambient air and $\delta^{13}C_p$ is that of the plant leaves. $\delta^{13}C_a$ measured during September 2017 and February 2018 were − 12.4 and − 11.5 ‰, respectively.

Sap flow (SF, $gH_2O/m^2\ s$) per individual per species was estimated according to the following equation (Granier, 1987):

$$SF = 119 \times \left[(\Delta T_{max} - \Delta T)/\Delta T\right]^{1.231} \quad (7)$$

where ΔT_{max} is the maximum value of ΔT logged at the no-transpiration period when SF was near zero (°C), and ΔT is the temperature difference between probes (°C).

Whole-individual daily transpiration (E_t, kgH_2O/day) per species was estimated by the following equation (Huang et al., 2011):

$$E_t = \sum_{t}\left[A_s \times \left(\frac{SF_{t_i} + SF_{t_{i+1}}}{2}\right) \times 15 \times 60\right]/1000 \quad (8)$$

where A_s (m^2) is sapwood area, t_i is a time in a day, and the interval between t_i and t_{i+1} is 15 min;/1000 is the constant for converting g to kg, and ×15 × 60 is the time constant for converting s^{-1} to day^{-1}.

Statistical analyses were conducted with IBM SPSS Statistics 25 (IBM Co., NY, USA). Differences in mean values of SWC of each soil depth and the $\delta^{18}O$ and $\delta^{2}H$ mean values of each source water (upper soil water, lower soil water, rainwater, and groundwater) were tested by one-way analysis of variance (ANOVA), followed by Tukey's honestly significant difference post-hoc test with $\alpha = 0.05$. One test was run separately for each parameter as the response (dependent) variable, while sampling locations and dates were set as the explanatory (independent) variables. Normality and homogeneity of variance assumptions within each data set were checked using Shapiro-Wilk's and Levene's tests, respectively. Additionally, differences in mean values of stem water $\delta^{18}O$ and $\delta^{2}H$, leaf $\delta^{13}C$, WUE_i, E_t, and proportions of each source water were tested with two-way ANOVA analyses after checking for data normality and homogeneity of variance assumptions. In these analyses, each parameter was considered as the dependent variable, while sampling sites (SDH and RDH), sampling seasons (dry and rainy), species, and their interaction were set as the fixed factors. Highly significant and moderately significant were defined as $P < 0.01$ and 0.05, respectively. Furthermore, linear regression analysis and the Pearson's correlation coefficient were used to determine correlations between groundwater proportion, WUE_i, and E_t for the species between the habitats and seasons. In each linear regression analysis performed using the enter method, physiological parameters and groundwater proportions were the dependent and independent variables, respectively.

3. Results

3.1. Seasonal distribution of rainfall and soil water

The total rainfall was 1334 mm throughout the study period of April 2017–March 2018. The highest monthly rainfall was 249 mm in September 2017, while the lowest was 10 mm in December 2017 (Fig. 3a). Approximately 85 % of the total rainfall occurred during the rainy season (April–October), 19 % of which occurred within the month prior to the first sampling period (late September; Fig. 3a). In contrast, approximately 15 % of the total rainfall occurred during the dry season (October–February), 1 % of which occurred within the month before the second sampling period (early March).

Soil layers in the SDH contained more SWC than those in the RDH all year round. The average values of SWC during the hydrological year 2017–2018 were 27 % and 23.9 % for soil layers in the SDH and RDH, respectively (Fig. 3b). Furthermore, lower soil layers had a higher SWC than upper soil layers in both habitats during the study period (28.7 % vs. 25.4 % in the SDH and 25.0 % vs. 22.8 % in the RDH; Fig. 3b). This implies that lower soil layers, compared to upper soil layers, in both habitats could supply more water in the environment to plants all year round. Peaks of SWC for both soil layers in both habitats occurred in May, June, and September, which coincided with the peaks of rainfall during these periods in the region. Additionally, the most significant decreases in the SWC of the soil layers in both habitats occurred during July and August, coinciding with significant rainfall gaps (summer droughts) during these 2 months. As shown in Fig. 3b, in September (late rainy season) and February (late dry season), the SWC of both soil layers in both habitats was higher and lower than their annual average, respectively. Thus, more water supply from both soil pools was available to plants in September than in February, mainly because of the significant rain inputs in September.

3.2. Temporal and spatial variations in isotopic ($\delta^{18}O$ and $\delta^{2}H$) signals of water sources

Isotopic signals of rainwater uptake were within the overall range of rainfall and interflow that occurred in September 2017 (i.e., rainfall and interflow that occurred approximately 1 month before the first sampling period, which shown as new (recent) rainwater in Figs. S1a and S2a). These signals fell on or near the local meteoric water line (LMWL; $\delta^{2}H = 8.33 \times \delta^{18}O + 19.4$ ‰), which is defined by Zhou and Li (2017) from the 6-year $\delta^{18}O$ and $\delta^{2}H$ records of rainfall in the same region. Isotopic signals associated with recent rainwater were also observed and confirmed by direct isotopic measurements made through 26 vertical profiles excavated across the shallow bedrock during June 2022 (mid-rainy season). These measurements showed that the signals of recent rain inputs during June 2022 were mainly held in the upper epikarst, and obviously differed from soil water and groundwater signals (see details in Supplementary material Fig. S3 and Note S2).

Soil water samples for both soil layers (between depths of 0–20 and 20–40 cm) deviated to the right of the LMWL during both seasons (Figs. S1 and S2), probably because of evaporative enrichment (Barnes and Turner, 1998). However, there were significant differences in the isotopic signals of soil water between both soil layers ($P < 0.05$). During both seasons and across both habitats, the lower soil layers showed more negative isotopic values than the upper soil layers, likely resulting from higher water retention and lower evaporative water losses (Barnes and Turner, 1998). Moreover, significant seasonal differences were observed in the soil water isotopic signals of both soil layers ($P < 0.01$). Both soil layers showed more negative isotopic values during the rainy season than during the dry season (Figs. S1 and S2). During the rainy season, the $\delta^{18}O$ and $\delta^{2}H$ values for most soil water samples from both soil layers across both habitats fell within the overall ranges of rainwater in August and July 2017 (i.e., rainfall that occurred two to three months before the first sampling period, which shown as old rainwater in Figs. S1a and S2a), while were far from those of groundwater samples. During the dry season, the $\delta^{18}O$ and $\delta^{2}H$ values of all soil water samples were within the overall ranges of rainwater in October and November 2017 (i.e., rainfall that occurred four to five months before the second sampling period), while differed from those of groundwater samples (Figs. S1b and S2b).

Groundwater (epikarst and phreatic water) samples fell on or close to the LMWL and within the overall ranges of rainwater in June and July 2017 (three to four months before sampling) during the rainy season (Figs. S1a and S2a), while they fell far below the LMWL and within the ranges of rainwater in October and November 2017 (four to five months before sampling) during the dry season (Figs. S1b and S2b). Overall, these results suggest that water in soil layers and groundwater pools primarily originates from (different) old rains rather than recent rains that may be stored in the upper epikarst.

3.3. Relationship between $\delta^{18}O$ and $\delta^{2}H$ signals of stem and source water

All four species assessed in both habitats showed significant seasonal variations in stem water isotopic signals ($P < 0.05$; Figs. 4, 5, S1, and S2), which were likely related to the seasonal variations in water availability of their potential sources. During the rainy season, isotopic signals for all the species, especially BP and CR species in both habitats, were close to the soil water and rainwater signals and were far from groundwater signals. This likely indicates that the species tend to rely more on water supplied from surface pools than deep pools during the period with high rain inputs (see next section). In contrast, during the dry season, isotopic signals for all the species, especially those in the RDH, were significantly close to groundwater signals than soil water signals. This indicates that the species tend to rely more on water supplied from deep pools than surface pools during the period with low rain inputs. Rainwater during the dry season (February 2018) was not sufficient to be measured and, thus, was not used as a potential water source for plant uptake.

3.4. Temporal and spatial patterns of plant water use

The relative shares of different water sources to the species' stem water varied significantly seasonally and between habitats ($P < 0.05$; Figs. 6, S5a–S12a). During the rainy season, all the species across the SDH relied significantly on soil water, while those across the RDH relied significantly on rainwater. Across the SDH, BP and CR species used higher shares of soil water during the rainy season (63 ± 15 % and 64 ± 18 %, respectively) compared to VC and FC species (56 ± 11 % and 52 ± 10 %, respectively). Interestingly, across the RDH, BP and CR species also used higher shares of rainwater during the rainy season (64 ± 24 % and 56 ± 19 %, respectively) compared to VC and FC species (49 ± 14 % and 46 ± 8 %, respectively). In contrast, during the dry season, all the species in both habitats, especially those in the RDH, relied largely on groundwater. Interestingly, VC and FC species in both habitats used greater shares of groundwater during the dry season (62 ± 8 % and 68 ± 9 % in the SDH, and 82 ± 9 % and 89 ± 5 % in the RDH, respectively) compared to BP and CR species in the corresponding habitats (46 ± 7 % and 51 ± 8 % in the SDH, and 69 ± 13 % and 75 ± 15 % in the RDH, respectively).

3.5. Temporal and spatial patterns of $\delta^{13}C$ and WUE_i

The mean leaf $\delta^{13}C$ and WUE_i values of all the species varied significantly seasonally and between habitats ($P < 0.05$; Figs. 7a,b, S5b − S12b). During both seasons, all the species in the SDH showed lower $\delta^{13}C$ and WUE_i values than the similar species in the RDH. Across both habitats, all the species showed significantly less $\delta^{13}C$ and WUE_i values during the rainy season than during the dry season. During the rainy season, BP and CR species in both habitats had lower $\delta^{13}C$ and WUE_i values (-32.54 and -32.19 ‰ in the SDH, and −31.58 and −31.39 ‰ in the RDH, respectively for $\delta^{13}C$; 62.54 and 66.31 mmol/mol in the SDH, and 72.73 and 74.82 mmol/mol in the RDH, respectively for WUE_i) compared to VC and FC species in the corresponding habitats (-31.33 and -31.59 ‰ in the SDH, and -30.88 and -31.21 ‰ in the RDH, respectively for $\delta^{13}C$; 75.43 and 72.68 mmol/mol in the SDH, and 80.23 and 76.74 mmol/mol in the RDH, respectively for WUE_i). In contrast, during the dry season, VC and FC species in both habitats had lower $\delta^{13}C$ and WUE_i values (-29.71 and -29.91 ‰ in the SDH, and -29.14 and -29.47 ‰ in the RDH, respectively for $\delta^{13}C$; 99.69 and 97.22 mmol/mol in the SDH, and 106.96 and 102.82 mmol/mol in the RDH, respectively for WUE_i) compared to BP and CR species in the corresponding habitats (-28.72 and -28.95 ‰ in the SDH, and -28.45 and -28.64 ‰ in the RDH, respectively for $\delta^{13}C$; 112.33 and 109.56 mmol/mol in the SDH, and 115.71 and 113.33 mmol/mol in the RDH, respectively for WUE_i).

3.6. Temporal and spatial patterns of E_t

The mean daily E_t values of all species also varied significantly seasonally and between habitats ($P < 0.05$; Figs. 7c, S5c–S12c). During both

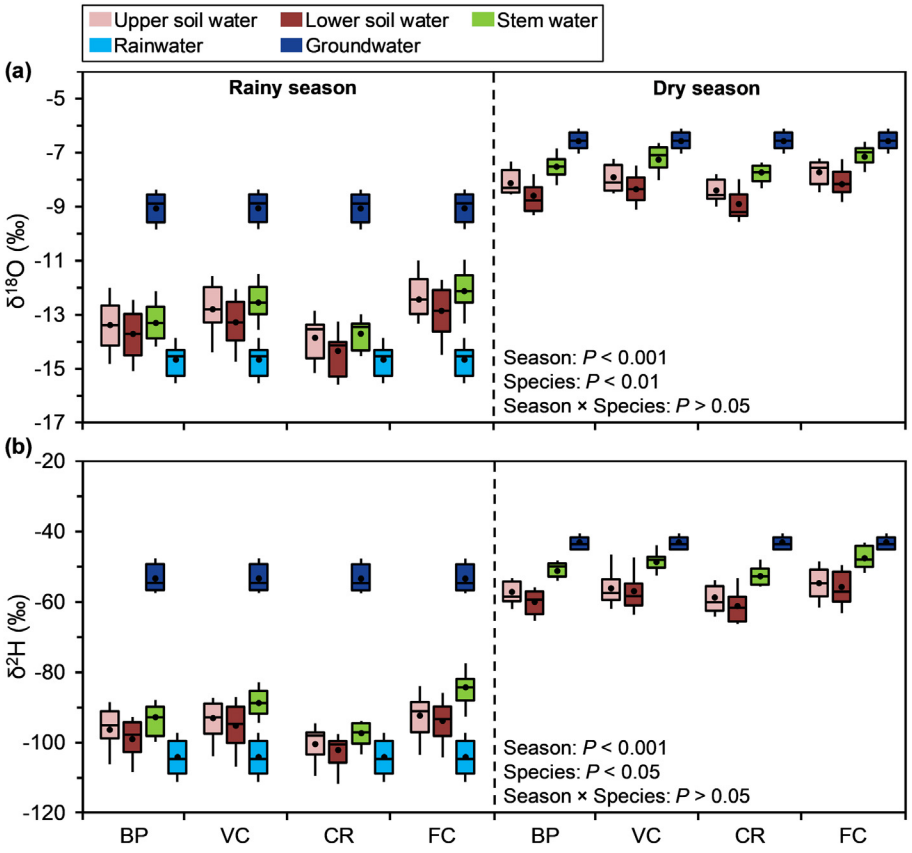

Fig. 4. Variations in the mean values of (a) $\delta^{18}O$ (‰) and (b) $\delta^{2}H$ (‰) from stem and source waters for four woody species growing across the soil-dominated habitat (SDH) during the rainy and dry seasons (September 2017 and February 2018). See Table 1 for species abbreviations.

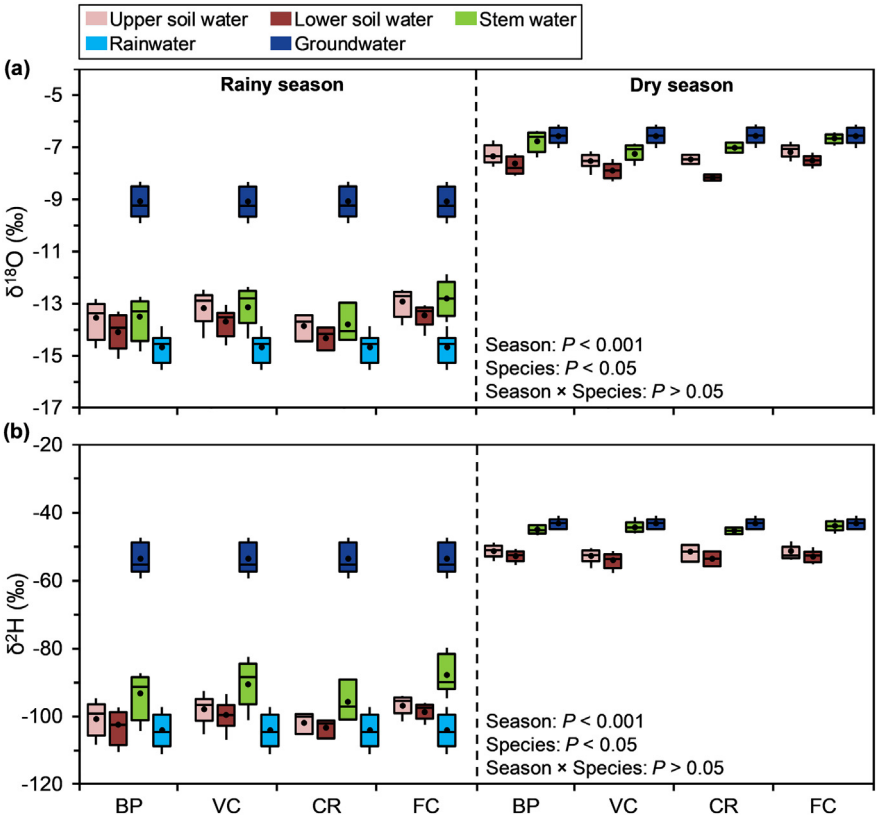

Fig. 5. Variations in the mean values of (a) $\delta^{18}O$ (‰) and (b) $\delta^{2}H$ (‰) from stem and source waters for four woody species growing across the rock-dominated habitat (RDH) during the rainy and dry seasons (September 2017 and February 2018). See Table 1 for species abbreviations.

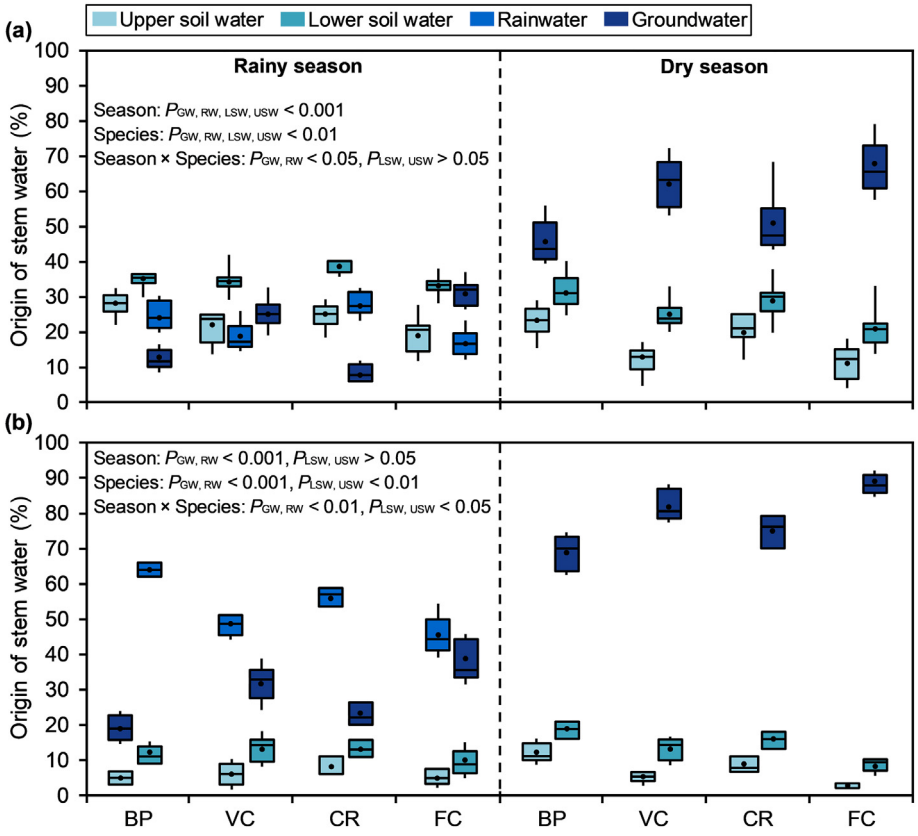

Fig. 6. Average relative shares (%) of potential water sources to the water within the stems of four woody species growing across the (a) soil-dominated habitat (SDH) and (b) rock-dominated habitat (RDH) during the rainy and dry seasons (September 2017 and February 2018). A dual isotope approach ($\delta^{18}O$ and $\delta^{2}H$) was used to estimate the shares of water sources. See Table 1 for species abbreviations. See also Supplementary Figs. S5a–S12a for observable differences between individuals of species across habitats during each season. GW, RW, LSW, and USW are groundwater, rainwater, lower soil water, upper soil water, respectively.

seasons, all four species in the SDH showed higher E_t compared to the similar species in the RDH. Across both habitats, all species showed higher E_t during the rainy season than during the dry season. During the rainy season, BP and CR species in both habitats had higher E_t (13.11 and 12.42 kgH_2O/day in the SDH, and 11.24 and 10.70 kgH_2O/day in the RDH, respectively) compared to VC and FC species in the corresponding habitats (10.24 and 10.84 kgH_2O/day in the SDH, and 9.35 and 10.02 kgH_2O/day in the RDH, respectively). In contrast, during the dry season, VC and FC species in both habitats had higher E_t (4.11 and 4.51 kgH_2O/day in the SDH, and 3.05 and 3.54 kgH_2O/day in the RDH, respectively) compared to BP and CR species in the corresponding habitats (2.24 and 2.65 kgH_2O/day in the SDH, and 1.93 and 2.17 kgH_2O/day in the RDH, respectively).

3.7. Variability of WUE_i and E_t associated with groundwater use

Linear regression analyses showed that WUE_i and E_t were positively and negatively associated with groundwater use for all species across both habitats during the rainy season and vice versa during the dry season ($P < 0.01$; Figs. 8, 9). According to Pearson's correlation coefficients between groundwater proportion, WUE_i, and E_t (Tables S4 and S5), and considering the maximum rooting depths (Table 1 and Section 4.2), two different patterns were observed between species across both habitats in both seasons. BP and CR species, which were grouped into the shallower-rooted species (SR species), compared to VC and FC species, which were grouped into the deeper-rooted species (DR species), showed lower WUE_i and higher E_t associated with lower groundwater use in both habitats during the rainy season and vice versa during the dry season. Conversely, VC and FC species, compared to BP and CR species, showed higher WUE_i and lower E_t associated with higher groundwater use in both habitats during the rainy season and vice versa during the dry season.

4. Discussion

4.1. Water uptake patterns influenced by seasonal variations in water availability

These findings reveal that the water uptake patterns of all four species vary significantly between seasons. During the rainy growing season, soil water and rainwater are the dominant water sources supplied for species in the SDH and RDH, respectively. During the dry season, groundwater is the dominant water source supplied for species, albeit with different shares, in both habitats. This indicates that the main water sources to support the growth of species come from surface pools, while the main water sources to maintain their function come from deep pools (Ryel et al., 2008, 2010). Similar instances of such seasonal shifts between growth and maintenance pools have been reported for native woody species in the same region (Liu et al., 2019; Wu et al., 2021) and in other karst regions (Rose et al., 2003; McCole and Stern, 2007; Nie et al., 2012). These studies have also highlighted that such a shift between the pools is due to an insufficient supply of soil water associated with a significant reduction of rain inputs during the dry season, which is consistent with the observations reported here.

Findings from this study also show that the water uptake patterns differ between habitats. Considering the similar climatic, topographical (slope and altitude), and geological conditions between the sampling sites, the differences could be mainly associated with the different pedological conditions between habitats. As previously mentioned (Section 2.2), the PAWS of soil in the RDH is considerably lower than that in the SDH due to the very poor soil cover, which largely limits the availability of soil water for species in the RDH.

This study also highlights that water uptake patterns differ between and within species. During both seasons and across both habitats, VC and FC species extracted higher shares of water from groundwater pools and

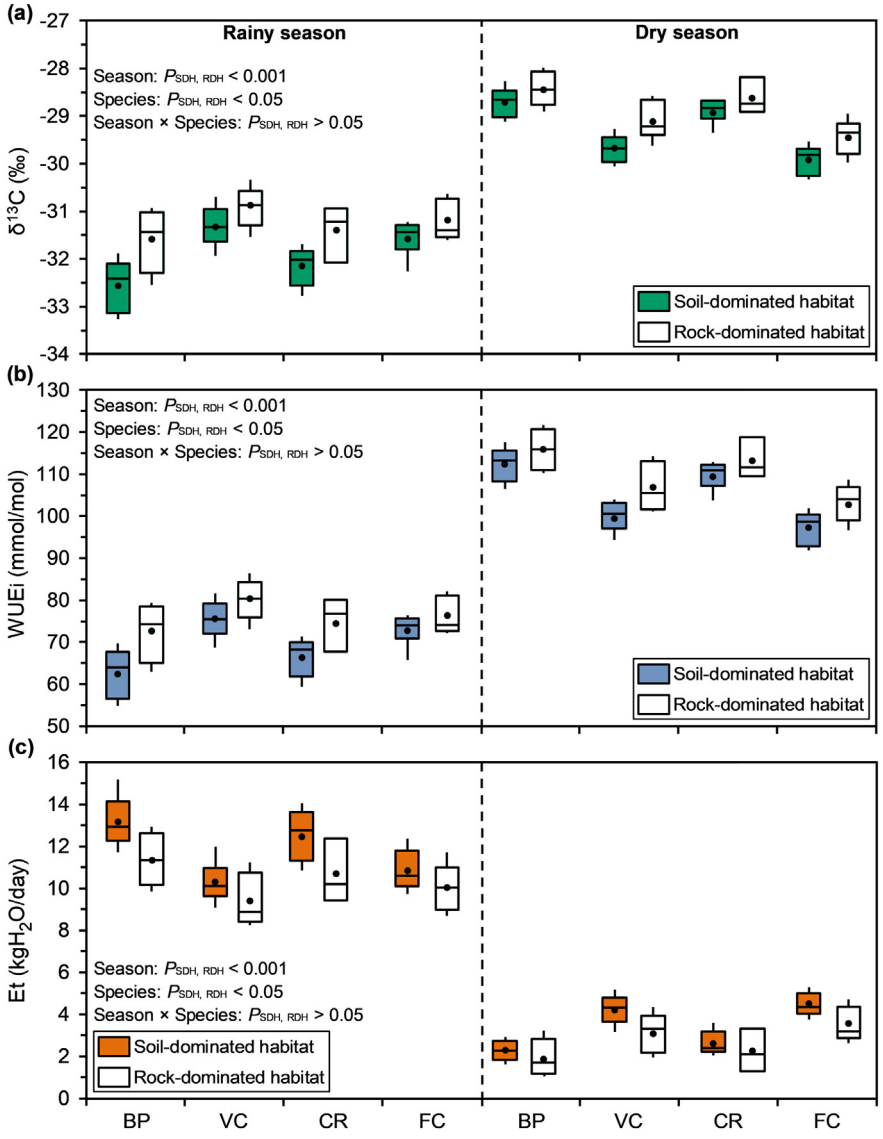

Fig. 7. Stand-level variations in the mean values of (a) leaf $\delta^{13}C$ (‰), (b) intrinsic water-use efficiency (WUE_i, mmol/mol), and (c) transpiration (E_t, kgH_2O/day) for four woody species growing across the soil- and rock-dominated habitats (SDH and RDH) during the rainy and dry seasons. See Table 1 for species abbreviations. See also Supplementary Figs. S5b,c to S12b,c for observable WUE_i and E_t differences between individuals of each species across habitats during each season.

lower from surface water pools compared to BP and CR species. This suggests a clear ecohydrological niche differentiation between species (Ding et al., 2021), which could be largely explained by their different rooting depths and physiological characteristics, as discussed in the next sections.

4.2. Rooting depth and water availability depth

A dimorphic root system could explain the above-mentioned seasonal shift between the growth and maintenance pools: a system of branched shallow and deep roots that play an essential role in depleting shallow- and deep-water reserves supplied in the environment, respectively (Dawson and Pate, 1996; Freschet et al., 2022). The presence of such a specialized root system is confirmed for all four species through the previous observations made in 46 pits excavated in the study area (Liu, 2018), the current observations made in roadcuts, and also inquiries from 13 local professional experienced drillers (Table 1). It was also reported in other field-based studies for many native karst species worldwide (White et al., 1985; Jackson et al., 1999; Querejeta et al., 2006; Nie et al., 2012, 2017; Nardini et al., 2016, 2020; Carrière et al., 2020). Furthermore, the mentioned seasonal shift also signals which part of the plant's roots might have been active between seasons. According to the IsotopeR results, it was assumed that the most active part of the roots during the rainy season is the shallow roots. Conversely, the more active part of the roots during the dry season is the deep roots. This hypothesis is in line with a field-based study done by Bleby et al. (2010). These researchers showed that throughout the drought, the water transport capacity of deep roots at depths of 20 m to meet the transpiration demand was five times higher than that of shallow roots at depths of 0–0.5 m, which then decreased significantly with the onset of rain to reach near zero.

Consistent with the findings of Ding et al. (2021), the most influential driver for the ecohydrological niche differentiation between species is the different rooting depths. Based on the field observations from the maximum rooting depth for each species, VC and FC species have substantially more developed roots in depth compared to BP and CR species, as the maximum rooting depths measured were between 9 and 36 m for VC and FC species and between 2 and 8 m for BP and CR species (Table 1). Therefore, combined with previous findings, this indicates that deeper-rooted species (DR species) tend to have deeper water uptake than shallower-rooted species (SR species). This is most likely because DR species, unlike SR species that only have access to shallow groundwater or epikarst water reserve,

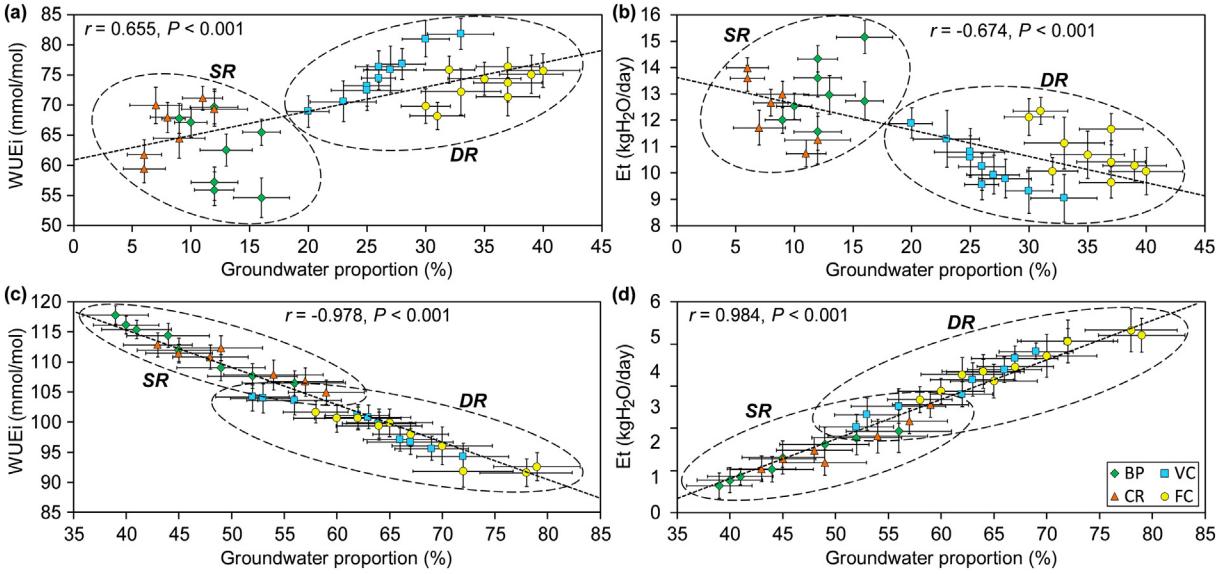

Fig. 8. Relationship between groundwater proportion (%) and (a, c) intrinsic water-use efficiency (WUE_i, mmol/mol), and (b, d) transpiration (E_t, kgH_2O/day) for four woody species growing across the soil-dominated habitat (SDH) during the (a, b) rainy (September 2017) and (c, d) dry seasons (February 2018). *Berchemia polyphylla* (BP) and *Citrus reticulate* (CR) were grouped into the shallower-rooted species (SR species), and *Viburnum chinshanense* (VC) and *Fraxinus chinensis* (FC) were grouped into the deeper-rooted species (DR species). Values are presented as the average ± SE.

also have access to deep groundwater or vadose and phreatic water reserve. This is in line with the findings of Jackson et al. (1999). They documented permanent access to groundwater reserves supplied in the karstified bedrock up to a maximum depth of 65 m for some native woody species.

4.3. Ecophysiological trade-offs governing transpiration in response to seasonal variations in water availability

The findings indicate that all the species across both habitats had lower $\delta^{13}C$ and WUE_i and higher E_t during the rainy season compared to the dry season, respectively. This could facilitate and prevent the further loss of H_2O molecules and the entry of CO_2 molecules through the leaf stomata during the rainy and dry seasons, respectively (Klein, 2014; Martínez-Vilalta and Garcia-Forner, 2017). The former feedback allows species to increase water and carbon demands because it is essential to maintain or increase the rate of photosynthesis and growth during the rainy growing period (Hubbard et al., 2001; Ainsworth and Rogers, 2007), and the latter feedback minimizes species demands because it is vital to reduce the drought stress, maintain functions, and survival during the dry period (Chaves et al., 2002; Tombesi et al., 2015). This investigation also revealed that during both seasons, all species in the RDH had higher $\delta^{13}C$ and WUE_i and lower E_t compared to the respective species in the SDH, respectively. This highlights that species in the RDH suffer from higher drought stress than those in the SDH year-round and, therefore, tend to minimize this stress and hydraulic risk through strict stomatal regulation (Klein et al., 2013; Garcia-Forner et al., 2016). These mechanisms typically occur at

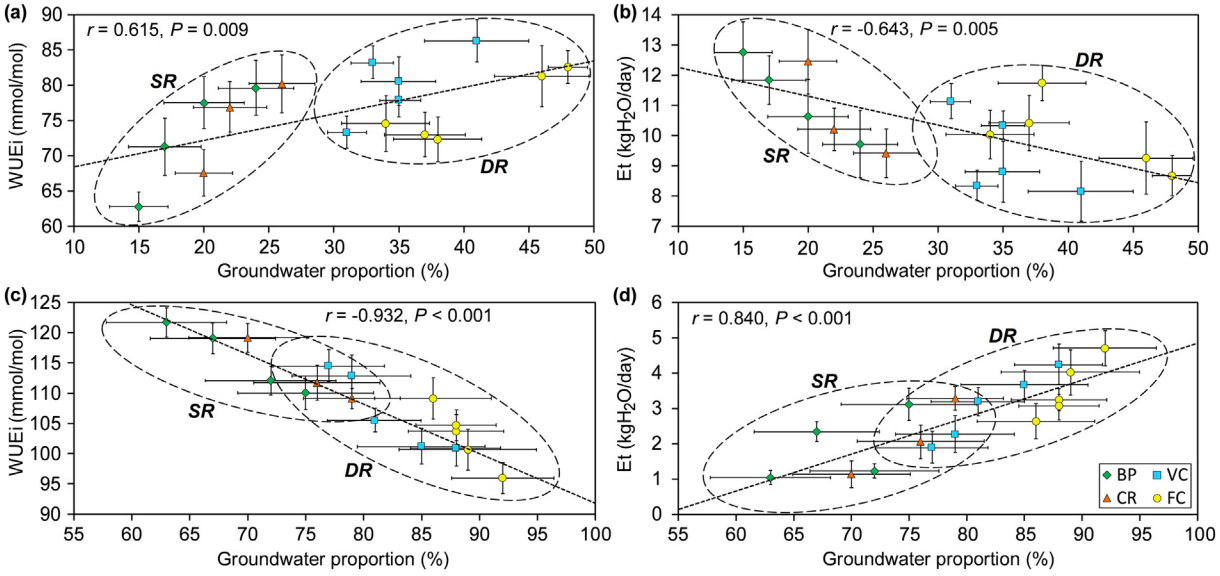

Fig. 9. Relationship between groundwater proportion (%) and (a, c) intrinsic water-use efficiency (WUE_i, mmol/mol), and (b, d) transpiration (E_t, kgH_2O/day) for four woody species growing across the rock-dominated habitat (RDH) during the (a, b) rainy (September 2017) and (c, d) dry seasons (February 2018). *Berchemia polyphylla* (BP) and *Citrus reticulate* (CR) were grouped into the shallower-rooted species (SR species), and *Viburnum chinshanense* (VC) and *Fraxinus chinensis* (FC) were grouped into the deeper-rooted species (DR species). Values are presented as the average ± SE.

the expense of reduced carbon assimilation and can lead to a reduction in the rate of photosynthesis as well as the growth rate during the growing period (Peñuelas et al., 2008; Obojes et al., 2018). Behzad et al. (2022) recently revealed that for two dominant drought-tolerant tree species in the same region, growth rates were significantly negative in response to all short- and long-term drought events between 1994 and 2011.

Other findings reveal that, for all the species across both habitats, WUE_i and E_t were positively and negatively associated with groundwater use during the rainy season and vice versa during the dry season (Figs. 8, 9). Therefore, despite the high water demand during the rainy growing season, species use less groundwater. Conversely, during the dry season and despite the low water demand, species use groundwater more. The following reasons could explain this behavioral inconsistency of species. Firstly, based on field observations, the abundance of root tips >1 mm in diameter for all four species in the surface zone, including the soil zone and soil-bedrock interface, was significantly higher during the rainy season than during the dry season. Therefore, this maximizes the species competitive capacity to collect more water from the surface than from the depth. Secondly, as Nardini et al. (2020) demonstrated, even if deep roots are sufficiently developed into groundwater pools, the bedrock matrix releases water into the roots at very slow rates. Therefore, water uptake from the surface is less time- and energy-consuming than from the depth. Thirdly, since water uptake is a transpiration-driven process (Ksenzhek and Volkov, 1998), less transpiration during the dry season could result in the formation of a lower hydrodynamic gradient, which limits the uptake of more water from potential pools, especially from groundwater pools (Bleby et al., 2010; Wu et al., 2021).

It was also revealed that, during the rainy season and across both habitats, DR species with higher groundwater use had higher $\delta^{13}C$ and WUE_i and lower E_t than SR species with lower groundwater use. This unexpected relationship is explained by the different distribution of shallow roots between the species. Field observations showed that the abundance of root tips >1 mm in diameter at the surface for DR species was significantly lower than for SR species. This minimizes the species competitive capacity to collect more water from surface pools as evidenced by the IsotopeR results. This could, in turn, force DR species to moderate their transpiration compared to SR species, which limits the formation of a greater hydrodynamic gradient to take up more water. Therefore, the higher capacity of species to extract more groundwater during the rainy growing season does not necessarily contribute to an increase in transpiration rate or a decrease in the drought stress level. Consistent with the hypothesis, during the dry season, DR species, compared to SR species, in both habitats had lower $\delta^{13}C$ and WUE_i and higher E_t associated with higher groundwater use. This allows DR species to make a greater hydrodynamic gradient to extract more groundwater and contribute to more efficient regulation of the transpiration rates under increased drought stress. These findings align with those of Carrière et al. (2020) and Ding et al. (2021). They similarly showed that water uptake depth coordinates with drought stress levels during drought periods for various species with deep roots in the KCZs.

5. Conclusions

The combination of various techniques in an extensive monitoring study conducted between two habitat types (SDH and DRH) during the rainy and dry seasons has provided insights into the water uptake and transpiration relationships of forest woody plants in a KCZ in China. This study highlights important temporal and spatial shifts in water uptake and transpiration patterns between and within species, which are attributed to: (1) heterogeneous distribution of water supply in the near-surface associated with changing rain inputs between seasons; (2) heterogeneous distribution of soil water supply associated with variable thickness of the soil between habitats; and (3) species-specific physiological behaviors and also heterogeneous distribution of roots between and within species. This study also reveals that water uptake and transpiration rates are comparatively high when and where plant drought stress is low, and conversely, they are comparatively low when and where plant drought stress is high. Taken together, this study shows to what extent forest woody plants in the KCZ with different physiological behaviors are flexible against the drought stresses mentioned here. Because of this flexibility, these plants manage water uptake strategies to support transpiration according to the water availability in the environment and develop growth and survival strategies in such a water-limited ecosystem.

CRediT authorship contribution statement

Hamid M. Behzad: Conceptualization, Methodology, Investigation, Sampling, Data curation, Formal analysis, Resources, Software, Visualization, Validation, Writing–original draft, Writing–review & editing, Supervision, Project administration, Funding acquisition. **Muhammad Arif** & **Alireza Kavousi**: Visualization, Methodology, Software, Writing–review & editing. **Shihui Duan**, **Min Cao**, & **Jiuchan Liu**: Resources, Sampling, Investigation. **Yongjun Jiang**: Methodology, Investigation, Resources, Writing–review & editing, Supervision, Project administration, Funding acquisition.

Data availability

Data will be made available on request.

Declaration of competing interest

The authors declare that they have no known competing financial interests or personal relationships that could have appeared to influence the work reported in this paper.

Acknowledgments

This research was supported by the Chongqing Municipal Science and Technology Commission Fellowship Fund (CSTC2021YSZX-JCYJX0005 and 2022YSZX-JCX0008CSTB), Innovation Research 2035 Pilot Plan of Southwest University (SWU-XDZD22003), and the National Key Research and Developmental Program of China (2016YFC0502306).

Appendix A. Supplementary data

Supplementary data to this article can be found online at https://doi.org/10.1016/j.scitotenv.2022.160424.

References

Ackerly, D.D., Kling, M., Clark, M., Papper, P.D., Oldfather, M.F., Flint, A.L., Flint, L.E., 2020. Topoclimates, refugia, and biotic responses to climate change. Front. Ecol. Environ. 18, 288–297.

Ainsworth, S., Rogers, A., 2007. The response of photosynthesis and stomatal conductance to rising [CO2]: mechanisms and environmental interactions. Plant Cell Environ. 30, 252–270.

Anderegg, W.R.L., Anderegg, L.D.L., Kerr, K.L., Trugman, A.T., 2019. Widespread drought-induced tree mortality at dry range edges indicates that climate stress exceeds species'compensating mechanisms. Glob. Chang. Biol. 25, 3793–3802.

Barbeta, A., Peñuelas, J., 2016. Sequence of plant responses to droughts of different timescales: lessons from holm oak (Quercus ilex) forests. Plant Ecol.Divers. 9, 321–338.

Barnes, C.J., Turner, J.V., 1998. Isotopic exchange in soil water. In: Kendall, C., McDonnell, J.J. (Eds.), Isotope Tracers in Catchment Hydrology. Elsevier, Amsterdam, pp. 137–164.

Behzad, H.M., Jiang, Y.J., Arif, M., Wu, C., He, Q.F., Zhao, H.J., Lv, T.R., 2022. Tunneling-induced groundwater depletion limits long-term growth dynamics of forest trees. Sci. Total Environ. 811, 152375.

Bleby, T.M., Mcelrone, A.J., Jackson, R.B., 2010. Water uptake and hydraulic redistribution across large woody root systems to 20 m depth. Plant Cell Environ. 33, 2132–2148.

Brum, M., Vadeboncoeur, M.A., Ivanov, V., Asbjornsen, H., Saleska, S., Alves, L.F., Penha, D., Dias, J.D., Arag˜ao, L.E.O.C., Barros, F., et al., 2019. Hydrological niche segregation defines forest structure and drought tolerance strategies in a seasonal Amazon forest. J. Ecol. 107, 318–333.

Cao, M., Wu, C., Liu, J.C., Jiang, Y.J., 2020. Increasing leaf δ13C values of woody plants in response to water stress induced by tunnel excavation in a karst trough valley: implication for improving water-use efficiency. J. Hydrol. 586, 124895.

Carrière, S.D., Ruffault, J., Pimont, F., Doussan, C., Simioni, G., Chalikakis, K., Limousin, J.-M., Scotti, I., Courdier, F., Cakpo, C.-B., Davi, H., Martin-StPaul, N., 2019. Impact of

local soil and subsoil conditions on inter-individual variations in tree responses to drought: insights from electrical resistivity tomography. Sci. Total Environ. 698, 134247.
Carrière, S.D., Martin-StPaul, N., Cakpo, C.B., Patris, N., Gillon, M., Chalikakis, K., Doussan, C., Olioso, A., Babic, M., Jouineau, A., Simioni, G., Davi, H., 2020. The role of deep vadose zone water in tree transpiration during drought periods in karst settings – insights from isotopic tracing and leaf water potential. Sci. Total Environ. 699, 1–10.
Chaves, M.M., Pereira, J.S., Maroco, J., Rodrigues, M.L., Ricardo, C.P., Osorio, L.M., Carvalho, I., Faria, T., Pinheiro, C., 2002. How plants cope with water stress in the field.Photosynthesis and growth. Ann. Bot. 89, 907–916.
Chen, H.S., Liu, J.W., Wang, K.L., Zhang, W., 2011. Spatial distribution of rock fragments on steep hillslopes in karst region of Northwest Guangxi,China. Catena 84, 21–28.
Chongqing Nanjiang Geological Engineering Survey and Design Institute (CNGESDI), 2015. Hydrogeological Long View Summary Report of the Geleshan Tunnel of the New Chengdu-Chongqing Passenger Rail Lines (in Chinese, unpublished report).
Craven, D., Hall, J.S., Ashton, M.S., Berlyn, G.P., 2013. Water-use efficiency and wholeplant performance of nine tropical tree species at two sites with contrasting water availability in Panama. Trees-Struct.Funct. 27, 639–653.
Dawson, T.E., Pate, J.S., 1996. Seasonal water uptake and movement in root systems of Australian phraeatophytic plants of dimorphic root morphology: a stable isotope investigation. Oecologia 107, 13–20.
Dawson, T.E., Hahm, W.J., Crutchfield-Peters, K., 2020. Digging deeper: what the critical zone perspective adds to the study of plant ecophysiology. New Phytol. 226, 666–671.
Deng, Y., Wu, S., Ke, J., Zhu, A.J., 2021. Effects of meteorological factors and groundwater depths on plant sap flow velocities in karst critical zone. Sci. Total Environ. 781, 146764.
Ding, Y.L., Nie, Y.P., Chen, H.S., Wang, K.L., Querejeta, J.I., 2021. Water uptake depth is coordinated with leaf water potential, water-use efficiency and drought vulnerability in karst vegetation. New Phytol. 229.
Du, S., Wang, Y.L., Kume, T., Zhang, J.G., Otsuki, K., Yamanaka, N., Liu, G.B., 2011. Sapflow characteristics and climatic responses in three forest species in the semiarid Loess Plateau region of China. Agric. For. Meteorol. 151, 1–10.
Ehleringer, J.R., Dawson, T.E., 1992. Water uptake by plants: perspectives from stable isotope composition. Plant Cell Environ. 15, 1073–1082.
Ehleringer, J.R., Roden, J., Dawson, T.E., 2000. Assessing ecosystem-level water relations through stable isotope ratio analyses. In: Sala, O.E., Jackson, R., Mooney, H.A., Howarth, R. (Eds.), Methods in Ecosystem Science. Springer, New York, pp. 181–214.
Estrada-Medina, H., Graham, R.C., Allen, M.F., Jimenez-Osornio, J.J., Robles-Casolco, S., 2013. The importance of limestone bedrock and dissolution karst features on tree root distribution in northern Yucatan,Mexico. Plant Soil 362, 37–50.
Fan, Y., 2015. Groundwater in the Earth's critical zone: relevance to large-scale patterns and processes. Water Resour. Res. 51, 3052–3069.
Farquhar, G.D., Richards, R.A., 1984. Isotopic composition of plant carbon correlates with water use efficiency of wheat genotypes. Aust. J. Plant Physiol. 11, 539–552.
Farquhar, G.D., Ehleringer, J.R., Hubick, K.T., 1989. Carbon isotope discrimination and photosynthesis. Annu. Rev. Plant Physiol. Plant Mol. Biol. 40, 503–537.
Freschet, G.T., Pagès, L., Iversen, C.M., Comas, L.H., Rewald, B., Roumet, C., Klimešová, J., Zadworny, M., Poorter, H., Postma, J.A., et al., 2022. A starting guide to root ecology: strengthening ecological concepts and standardising root classification, sampling, processing and trait measurements. New Phytol. 3, 973–1122.
Garcia-Forner, N., Adams, H.D., Sevanto, S., Collins, A.D., Dickman, L.T., Hudson, P.J., Zeppel, M.J.B., Jenkins, M.W., Powers, H., Martínez-Vilalta, J., et al., 2016. Responses of two semiarid conifer tree species to reduced precipitation and warming reveal new perspectives for stomatal regulation. Plant Cell Environ. 39, 38–49.
Gonfiantini, R., 1978. Standards for stable isotope measurements in natural compounds. Nature 271, 534–536.
Granier, A., 1987. Evaluation of transpiration in a Douglas-fir stand by means of sap flow measurements. Tree Physiol. 3, 309–320.
Gregory, L., Wilcox, B.P., Shade, B., Munster, C., Owens, K., Veni, G., 2009. Large-scale rainfall simulation over shallow caves on karst shrublands. Ecohydrology 2, 72–80.
Hahm, W.J., Rempe, D.M., Dralle, D.N., Dawson, T.E., Lovill, S.M., Bryk, A.B., Bish, D.L., Schieber, J., Dietrich, W.E., 2019. Lithologically controlled subsurface critical zone thickness and water storage capacity determine regional plant community composition. Water Resour. Res. 55, 3028–3055.
Hahm, W.J., Dralle, D.N., Sanders, M., Bryk, A.B., Fauria, K.E., Huang, M.H., Rasmussen, B.H., Nelson, M.D., Pedrazas, M.A., Schmidt, L., et al., 2022. Bedrock vadose zone storage dynamics under extreme drought: consequences for plant water availability, recharge, and runoff. Water Resour. Res. 58, e2021WR031781.
Hopkins, J.B., Ferguson, J.M., 2012. Estimating the diets of animals using stable isotopes and a comprehensive Bayesian mixing model. PLoS One 7 (1), e28478.
Huang, Y.Q., Li, X., Zhang, Z.F., He, C.X., Zhao, P., You, Y., Mo, L., 2011. Seasonal changes in cyclobalanopsis glauca transpiration and canopy stomatal conductance and their dependence on subterranean water and climatic factors in rocky karst terrain. J. Hydrol. 402, 135–143.
Hubbard, R.M., Ryan, M.G., Stiller, V., Sperry, J.S., 2001. Stomatal conductanceand photosynthesis vary linearly with plant hydraulic conductance inponderosa pine. Plant Cell Environ. 24, 113–121.
IAEA, 2014. IAEA/GNIP precipitation sampling guide [WWW Document]. URL http://www-naweb.iaea.org/napc/ih/documents/other/gnip_manual_v2.02_en_hq.pdf.
Jackson, R.B., Moore, L.A., Hoffmann, W.A., Pockman, W.T., Linder, C.R., 1999. Ecosystem rooting depth determined with caves and DNA. Proc. Natl. Acad. Sci. U. S. A. 96, 11387–11392.
Jiang, P.P., Wang, H.M., Meinzer, F.C., Kou, L., Dai, X.Q., Fu, X.O., 2020. Linking reliance on deep soil water to resource economy strategies and abundance among coexisting understorey shrub species in subtropical pine plantations. New Phytol. 225, 222–233.
Klein, T., 2014. The variability of stomatal sensitivity to leaf water potential across tree species indicates a continuum between isohydric and anisohydric behaviours. Funct. Ecol. 28, 1313–1320.
Klein, T., Cohen, S., Yakir, D., 2011. Hydraulic adaptations underlying drought resistance of Pinus halepensis. Tree Physiol. 31, 637–648.
Klein, T., Shpringer, I., Fikler, B., Elbaz, G., Cohen, S., Yakir, D., 2013. Relationships between stomatal regulation, water-use, and water-use efficiency of two coexisting key Mediterranean tree species. For. Ecol. Manag. 302, 34–42.
Ksenzhek, O.S., Volkov, A.G., 1998. Plant Energetics. Elsevier Inc., pp. 243–266.
Leo, M., Oberhuber, W., Schuster, R., Grams, T.E.E., Matyssek, R., Wieser, G., 2014. Evaluating the effect of plant water availability on inner alpine coniferous trees based on sap flow measurements. Eur. J. For. Res. 133, 691–698.
Li, J., Hong, A.H., Yuan, D.X., Jiang, Y.J., Deng, S.J., Cao, C., Liu, J., 2021. A new distributed karst-tunnel hydrological model and tunnel hydrological effect simulations. J. Hydrol. 593, 125639.
Liu, J., 2018. Eological Research on Karst Forest of Zhongliang Mountain, Southwest China. Southwest University, Chongqing (in Chinese).
Liu, D.D., She, D.L., 2020. The effect of fracture properties on preferential flow in carbonate-derived laterite from karst mountainous agroforestry lands. Soil Tillage Res. 203, 104670.
Liu, J.C., Shen, L.C., Wang, Z.X., Duan, S.H., Wu, W., Peng, X.Y., Wu, C., Jiang, Y.J., 2019. Response of plants water uptake patterns to tunnels excavation based on stable isotopes in a karst trough valley. J. Hydrol. 571, 485–493.
Liu, C., Huang, Y., Wu, F., Liu, W., Ning, Y., Huang, Z.R., Tang, S.Q., Liang, Y., 2021. Plant adaptability in karst regions. J. Plant Res. 134, 889–906.
Liu, W.N., Chen, H.S., Zou, Q.Y., Nie, Y.P., 2021. Divergent root water uptake depth and coordinated hydraulic traits among typical karst plantations of subtropical China: implication for plant water adaptation under precipitation changes. Agric. Water Manag. 249, 106798.
Lv, Y.X., Jiang, J., Chen, L., Hu, W., Jiang, Y.J., 2022. Elaborate simulation and predication of the tunnel drainage effect on karst groundwater field and discharge based on visual MODFLOW. J. Hydrol. 612, 128023.
Martínez-Vilalta, J., Garcia-Forner, N., 2017. Water potential regulation, stomatal behaviour and hydraulic transport under drought: deconstructing the iso/anisohydric concept. Plant Cell Environ. 40, 962–976.
Maxwell, T.M., Silva, L.C.R., Horwath, W.R., 2018. Integrating effects of species composition and soil properties to predict shifts in montane forest carbon–water relations. Proc. Natl. Acad. Sci. 115, E4219–E4226.
McCole, A.A., Stern, L.A., 2007. Seasonal water use patterns of Juniperus ashei on the Edwards Plateau, Texas, based on stable isotopes in water. J. Hydrol. 342, 238–248.
McDowell, N.G., Beerling, D.J., Breshears, D.D., Fisher, R.A., Raffa, K.F., Stitt, M., 2011. The interdependence of mechanisms underlying climate-driven vegetation mortality. Trends Ecol.Evol. 26, 523–532.
McLaughlin, B.C., Ackerly, D.D., Klos, P.Z., Natali, J., Dawson, T.E., Thompson, S.E., 2017. Hydrologic refugia, plants, and climate change. Glob. Chang. Biol. 23, 2941–2961.
Millar, C., Pratt, D., Schneider, D.J., McDonnell, J.J., 2018. A comparison of extraction systems for plant water stable isotope analysis. Rapid Commun. Mass Spectrom. 32, 1031–1044.
Nardini, A., Casolo, V., Borgo, A.D., Savi, T., Stenni, B., Bertoncin, P., Zini, L., McDowell, N.G., 2016. Rooting depth, water relations and non-structural carbohydrate dynamics in three woody angiosperms differentially affected by an extreme summer drought. Plant Cell Environ. 39, 618–627.
Nardini, A., Petruzzellis, F., Marusig, D., Tomasella, M., Natale, S., Altobelli, A., Calligaris, C., Floriddia, G., Cucchi, F., Forte, E., Zini, L., 2020. Water 'on the rocks': a summer drink for thirsty trees? New Phytol. 229, 199–212.
Nie, Y.P., Chen, H.S., Wang, K.L., Yang, J., 2012. Water source utilization by woody plants growing on dolomite outcrops and nearby soils during dry seasons in karst region of southwest China. J. Hydrol. 420–421, 264–274.
Nie, Y.P., Chen, H.S., Ding, Y.L., Yang, J., Wang, K.L., 2017. Comparison of rooting strategies to explore rock fractures for shallow soil-adapted tree species with contrasting aboveground growth rates: a greenhouse microcosm experiment. Front. Plant Sci. 8, 1651.
Nie, Y.P., Chen, H.S., Ding, Y.L., Zou, Q.Y., Ma, X.Y., Wang, K.L., 2019. Qualitative identification of hydrologically different water sources used by plants in rock-dominated environments. J. Hydrol. 573, 386–394.
O'Leary, M.H., 1981. Carbon isotope fractionation in plants. Phytochemistry 20, 553–567.
Obojes, N., Meurer, A., Newesely, C., Tasser, E., Oberhuber, W., Mayr, S., Tappeiner, U., 2018. Water stress limits transpiration and growth of European larch up to the lower subalpine belt in an inner-alpine dry valley. New Phytol. 220, 460–475.
Orlowski, N., Frede, H.-G., Brüggemann, N., Breuer, L., 2013. Validation and application of a cryogenic vacuum extraction system for soil and plant water extraction for isotope analysis. J.Sensors Sensor Syst. 2, 179–193.
Peñuelas, J., Hunt, J.M., Ogaya, R., Jump, A.S., 2008. Twentieth century changes of tree-ring δ13C at the southern range-edge of Fagus sylvatica: increasing water-use efficiency does not avoid the growth decline induced by warming at low altitudes. Glob. Chang. Biol. 14, 1076–1088.
Querejeta, J., Estrada-Medina, H., Allen, M.F., Jiménez-Osornio, J.J., Ruenes, R., 2006. Utilization of bedrock water by Brosimum alicastrum trees growing on shallow soil atop limestone in a dry tropical climate. Plant Soil 287, 187–197.
Richter, D., Billings, S.A., 2015. 'One physical system': Tansley's ecosystem as Earth's critical zone. New Phytol. 206, 900–912.
Rose, K.L., Graham, R.C., Parker, D.R., 2003. Water source utilization by Pinus jeffreyi and Arctostaphylos patula on thin soils over bedrock. Oecologia 134, 46–54.
Ryel, R.J., Ivans, C.Y., Peek, M.S., Leffler, A.J., 2008. Functional differences in soil water pools: a new perspective on plant water use in water-limited ecosystems. Prog.Bot. 69, 397–422.
Ryel, R.J., Leffler, A.J., Ivans, C.Y., Peek, M.S., Caldwell, M.M., 2010. Functional differences in water-use patterns of contrasting life forms in great basin steppelands. Vadose Zone J. 9, 548–560.
Schultz, N.M., Griffis, T.J., Lee, X., Baker, J.M., 2011. Identification and correction of spectral contamination in 2H/1H and 18O/16O measured in leaf, stem, and soil water. Rapid Commun. Mass Spectrom. 25, 3360–3368.

Schwarcz, H.P., 1991. Some theoretical aspects of isotope paleodiet studies. J. Archaeol. Sci. 18, 261–275.

Schwinning, S., 2020. A critical question for the critical zone: how do plants use rock water? Plant Soil 454, 49–56.

Teodoro, G.S., Lambers, H., Nascimento, D.L., Costa, P.D.B., Flores-Borges, D.N.A., Abrahao, A., Mayer, J.L.S., Sawaya, A.C.H.F., Ladeira, F.S.B., Abdala, D.B., et al., 2019. Specialized roots of velloziaceae weather quartzite rock while mobilizing phosphorus using carboxylates. Funct. Ecol. 33, 762–773.

Tombesi, S., Nardini, A., Frioni, T., Soccolini, M., Zadra, C., Farinelli, D., Poni, S., Palliotti, A., 2015. Stomatal closure is induced by hydraulic signals and maintained by ABA in drought-stressed grapevine. Sci. Rep. 5, 12449.

U. S. Department of Agriculture (USDA), Natural Resources Conservation Service (NRCS), 2012. Chapter 3, engineering classification of earth materials. National Engineering Handbook, Part 631, Dams. Washington, DC.

Wang, J., Fu, B., Lu, N., Zhang, L., 2017. Seasonal variation in water uptake patterns of three plant species based on stable isotopes in the semi-arid Loess Plateau. Sci. Total Environ. 609, 27–37.

Wang, J., Wen, X.F., Lyu, S.D., Guo, Q.J., 2021. Transition in multi-dimensional leaf traits and their controls on water use strategies of co-occurring species along a soil limiting-resource gradient. Ecol. Indic. 128, 107838.

Wassenaar, L.I., Coplen, T.B., Aggarwal, P.K., 2014. Approaches for achieving long-term accuracy and precision of δ18O and δ2H for waters analyzed using laser absorption spectrometers. Environ.Sci.Technol. 48, 1123–1131.

West, A.G., Patrickson, S.J., Ehleringer, J.R., 2006. Water extraction times for plant and soil materials used in stable isotope analysis. Rapid Commun. Mass Spectrom. 20, 1317–1321.

West, A.G., Goldsmith, G.R., Brooks, P.D., Dawson, T.E., 2010. Discrepancies between isotope ratio infrared spectroscopy and isotope ratio mass spectrometry for the stable isotope analysis of plant and soil waters. Rapid Commun. Mass Spectrom. 24, 1948–1954.

White, J.W.C., Cook, E.R., Lawrence, J.R., Broecker, W.S., 1985. The D/H ratios of sap in trees: implications for water sources and tree ring D/H ratios. Geochim. Cosmochim. Acta 49, 237–246.

Wu, H.W., Li, X.Y., Jiang, Z.Y., Chen, H.Y., Zhang, C.C., Xiao, X., 2016. Contrasting water use pattern of introduced and native plants in an alpine desert ecosystem, Northeast Qinghai-Tibet Plateau,China. Sci. Total Environ. 542, 182–191.

Wu, Z., Behzad, H.M., He, Q.F., Wu, C., Bai, Y., Jiang, Y.J., 2021. Seasonal transpiration dynamics of evergreen Ligustrum lucidum linked with water source and water-use strategy in a limestone karst area, southwest China. J. Hydrol. 597, 126199.

Yang, J., Nie, Y.P., Chen, H.S., Wang, S., Wang, K.L., 2016. Hydraulic properties of karst fractures filled with soils and regolith materials: implication for their ecohydrological functions. Geoderma 276, 93–101.

Zhao, Y., Wang, L., 2018. Plant water use strategy in response to spatial and temporal variation in precipitation patterns in China: a stable isotope analysis. Forests 9, 123.

Zhou, J.-L., Li, T.-Y., 2017. A tentative study of the relationship between annual δ18O & δD variations of precipitation and atmospheric circulations–a case from southwest China. Quat. Int. 479, 117–127.